View metadata, citation and similar papers at core.ac.uk
brought to you by CORE
provided by AJOL - African Journals Online

Benguela Dynamics
Pillar, S. C., Moloney, C. L., Payne, A. I. L. and F. A. Shillington (Eds). *S. Afr. J. mar. Sci. 19: 99–112*
1998

SATELLITE COMPARISON OF THE SEASONAL CIRCULATION IN THE BENGUELA AND CALIFORNIA CURRENT SYSTEMS

P. T. STRUB, F. A. SHILLINGTON†, C. JAMES* and S. J. WEEKS†*

Satellite surface height and surface temperature fields are used to examine the seasonal surface circulation in the Benguela and California Current systems. In the California Current system, an equatorward jet develops in spring and summer near to the coast, with a latitudinal structure that responds to the equatorward longshore winds. This jet moves offshore from spring to autumn and contributes eddy kinetic energy to the deep ocean. In the Benguela system north of 32°S, winds are upwelling-favourable and currents are equatorward all year, but stronger in summer. The current strengthens in summer, when water parcels with high steric heights move into the region offshore of the jet from the Agulhas Retroflection area at the same time that steric heights next to the coast drop as a result of coastal upwelling. Off the Cape (32–34°S), winds and currents are more seasonal. The *Geosat* altimeter fields do not resolve the equatorward flow along the SST front next to the coast in spring and summer, but pick up strong equatorward flow off the Cape in autumn and winter, after the front moves offshore.

Upwelling systems in eastern boundary currents have been compared by a number of authors with respect to their forcing, dynamics and biological characteristics (Parrish *et al*. 1983, Smith 1983, Bakun and Nelson 1991, Hutchings 1992, Lentz 1992). When the dynamics of the regions over the shelves (often within 20–50 km of the coast) are examined, the systems exhibit a fair degree of similarity. The upper ocean circulation in these regions follows simple Ekman dynamics to lowest order (Lentz 1992). Differences are found in the location of return, onshore flow. In some regions, this takes place in the middle of the water column, under a shallow Ekman layer, whereas in other systems the onshore flow is found in a bottom boundary layer (Smith 1983).

When the larger scale circulation of these eastern boundary currents is considered, each appears to have a unique way of interacting with the surrounding, basin-scale circulation. In this study, the large-scale circulation of the California Current system is compared with that of the Benguela Current system, using satellite altimeter measurements of surface height and satellite measurements of surface temperature. Winds from the European Community Mesoscale Weather Forecast (ECMWF) model are used to describe mean monthly longshore surface wind forcing.

The California Current flows equatorwards from approximately 50 to 20°N, connecting the eastward West Wind Drift at 50°N to the westward North Equatorial Current. Hickey (1998) reviews the circulation in the California Current system in detail. The northern region (Oregon and Washington, north of about 43°N) has a straight coast and two main sources of freshwater input (the Strait of Juan de Fuca at 48–49°N and the Columbia River at 46°N). Wind forcing in this region is moderately upwelling-favourable in summer and strongly downwelling-favourable in winter. The middle region (35–43°N) has a number of capes and the strongest seasonal contrast in winds, with strong and persistent upwelling-favourable winds in summer and poleward, downwelling-favourable winds during storms in winter. The winter winds drive a poleward Davidson Current in the 100 km close to the coast, inshore of continued equatorward flow farther offshore. The influence of storms decreases south of approximately 37°N, where monthly mean winds remain upwelling-favourable all year (Bakun and Nelson 1991). The coast turns sharply eastwards at 35°N, forming the Southern California Bight between 32 and 35°N, a region sheltered from the strong wind forcing found elsewhere in the system. Off Baja California, between 22 and 32°N, winds are stronger than in the Bight and upwelling-favourable year round, although weaker than the summer winds off northern California. Several large capes are also found along the Baja coastline.

The Benguela Current flows equatorwards from the western tip of Africa near 34°S to the Angola Front at approximately 15°S, where it flows offshore and to the west (Shannon 1985, Shillington 1998). Although various authors have identified a number of upwelling "cells" in the Benguela system (Lutjeharms and Meeuwis 1987), for simplicity, three coastal capes that are areas of intense upwelling are identified: Cape Frio in the north (16–19°S); the coastal area off Lüderitz (25–28°S); and the area between Cape

* College of Oceanographic and Atmospheric Sciences, Oregon State University, Corvallis, Oregon, 97331-5503, USA.
Email: tstrub@oce.orst.edu
† Department of Oceanography, University of Cape Town, Rondebosch 7701, South Africa.

Manuscript received: January 1997

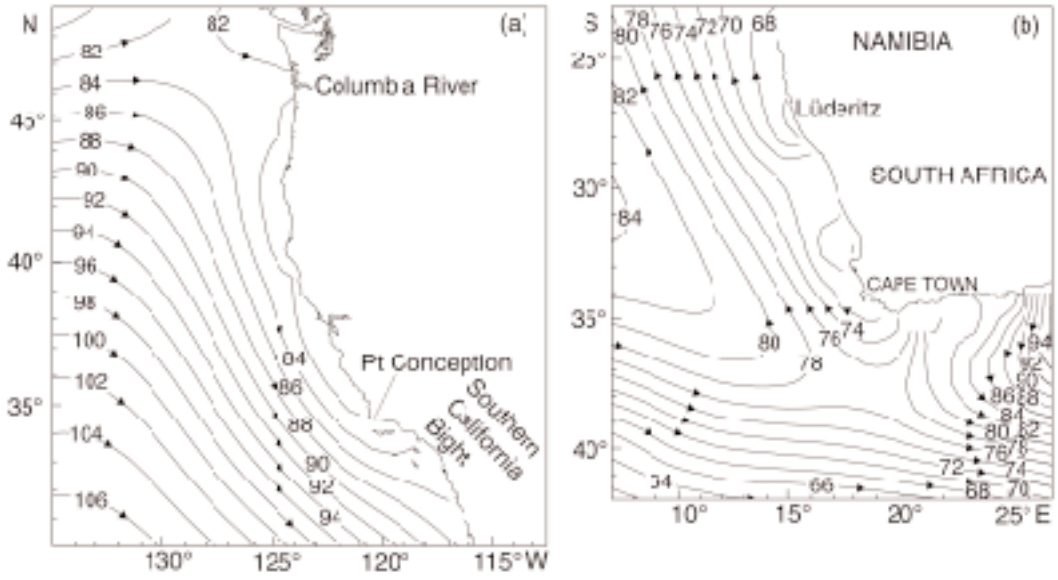

Fig. 1: Long-term average dynamic heights relative to 500 m for (a) the California Current region and (b) the Benguela system, calculated from the mean temperature and salinity data of Levitus and Gelfeld (1992). Contour intervals are 2 cm

Columbine and the Cape Peninsula in the south (33–34°S), which is referred to here as the "Cape Region." Other upwelling centres are recognized between these capes, such as Hondeklip Bay (around 30°S). In comparison to other eastern boundary currents, the unique features of the Benguela are that the poleward limits of the coast begin at only 34°S and that the inflow comes not just from the eastward equivalent of the West Wind Drift (the South Atlantic Current), but from the much more energetic Agulhas Retroflection, with extremely strong eddies spawned in the Retroflection Area (weakly represented in the climatological mean at 37°S, 23°E). For comparison to the California Current system, it is as if the entire North American continent were removed north of Point Conception (34–35°N) to the Carolinas, while the width of the continent was reduced, allowing the Gulf Stream to loop westwards and deposit anticyclonic eddies offshore of Baja California. In other words, the equivalent of the northern and central regions of the California Current system are missing from the Benguela system.

DATA AND METHODS

The patterns of oceanic circulation presented in this paper are derived from altimeter surface height fields. These include the height associated with geostrophic currents and the height associated with the marine geoid caused by the local gravity field. Because the marine geoid is poorly known, a two-year mean altimeter height field has been subtracted from each field to eliminate the unknown geoid, which otherwise dominates the signal. This also eliminates the height associated with the mean velocity field, leaving height anomalies. Contours of altimeter height anomalies are approximate streamlines of the temporally varying geostrophic velocity fields. The altimeter data used in this study are primarily from the *Geosat* altimeter. TOPEX altimeter data are used to provide a better look at velocity variability over a three-year period, but are too coarsely spaced to produce contoured height fields on scales small enough to resolve the features of interest in these systems.

The *Geosat* altimeter data are from the first two years of the 17-day exact repeat mission, beginning in November 1986. TOPEX data from the first three years of the TOPEX/POSEIDON mission (beginning October 1992) are used to show the seasonal changes in velocity variance. Data from the POSEIDON altimeter are not used. Data from both *Geosat* and TOPEX altimeters have been regridded to positions every 6–7 km along sub-satellite tracks and corrected for environmental errors at the Jet Propulsion Laboratory (JPL, Zlotnicki *et al*. 1990).

A climatological mean dynamic height field is

calculated (relative to 500 m) from the climatological temperature and salinity fields of Levitus and Gelfeld (1992) and added to the data to partially make up for the loss of the mean circulation. These climatological mean dynamic height fields are shown in Figure 1, depicting slow and broad equatorward flow in the eastern boundary currents, downstream of the west wind drift that flows into the poleward ends of the currents. The Benguela Current also includes input from the Agulhas Current, which appears to flow southwards in an unrealistic manner near 35°S, 26°E in the climatological height field. This feature has no effect on this analysis of the Benguela off the west coast of South Africa.

The contoured altimeter height fields were combined with SST fields from the Advanced Very High Resolution Radiometer (AVHRR). These show the location of the temperature fronts, which are better indicators of jets within 50 km of the coast than the altimeter contours. AVHRR data used to show the seasonal cycle of SST over the California Current were obtained from the JPL, consisting of monthly global fields with 18 km resolution. Individual AVHRR images, with approximately 1 km resolution, are also used to show snapshots of the SST field over the California Current. The individual images use only Channel 4 radiance temperatures. AVHRR data for specific periods in 1986–87 used over the Benguela system are weekly warmest pixel composites of multi-channel SST (obtained from the Joint Research Centre, European Commission, Ispra, Italy), with a resolution of 4 km.

Two-dimensional horizontal fields of sea surface height are constructed from the altimeter data using the method of successive corrections (Bratseth 1986). This method of objective analysis forms a linear-weighted combination of all available data within time and space windows around each point in a regular grid. During each of four iterations, the spatial scale is reduced from an initial value of 1.25 degrees to 0.5 degrees (Vazquez *et al.* 1990). The net result is to produce a smooth field that has values everywhere that data exist within the largest spatial window, with refined resolution in regions where the observations are dense.

RESULTS AND DISCUSSION

Wind stress forcing

The individual monthly mean longshore wind stresses for the *Geosat* period are calculated from ECMWF winds over each system (Fig. 2). These show maximum upwelling conditions (equatorward winds) in summer for each hemisphere at latitudes of approximately 40°N and 27°S. The northern half of the California Current is subjected to downwelling (poleward winds) for 3–7 months, mainly between November and February. In contrast, only the Cape Region south of 32°S experiences significant mean monthly downwelling-favourable winds for several months in May–July. In the California Current system, there is a rapid spring transition to upwelling-favourable equatorward winds in April 1987, after strong poleward winds as a result of storms in March. The situation is different in 1988, when stronger upwelling conditions begin first south of 43°N in February–March, but do not extend north of 43°N until June. In the Benguela system, only the Cape Region experiences a mean wind reversal over monthly scales and the transition is not as dramatic.

Circulation in the California Current

In Figure 3, the seasonal cycle of sea surface heights (two years of altimeter data plus the long-term climatological mean from Fig. 1) is overlaid on the seasonal cycle of SST. The seasonal cycle of altimeter heights in the Figure is not the simple mean of all data from each season. When the simple mean is constructed for each season, alternating bands of high and low regions occur next to the coast in most seasons. These are interpreted as spurious features caused by the large number of data dropouts on the tracks which move from land to ocean off the west coast of the USA. To filter out incoherent variability in the data, Empirical Orthogonal Functions (EOFs) are formed for the altimeter data and the first six EOFs are used to reconstruct the time-series. All six EOFs are needed to recover approximately 40% of the original variance in the time-series, because of the high level of noise in the *Geosat* data. Seasonal cycles formed from the reconstructed time-series are not as strongly contaminated by the spurious highs and lows along the coast.

The winter pattern shows equatorward flow in the California Current system far offshore, with high sea levels next to the coast between 39 and 46°N, corresponding to the poleward Davidson Current. Tide-gauge data analysed previously show high sea levels extending along the entire coast in early winter. Therefore, for that period, it is believed that the altimeter depiction of the Davidson Current in winter is correct north of 39°N, but other data suggest that poleward flow should extend as far south as 33°N (Lynn and Simpson 1987). In late winter and early spring, tide-gauge data show that lower sea levels and equatorward flow appear first in the south (Lynn and Simpson 1987, Strub *et al.* 1987, Strub and James 1988). In Figure 3a, the equatorward flow south of 39°N in winter is more characteristic of early spring. At some point

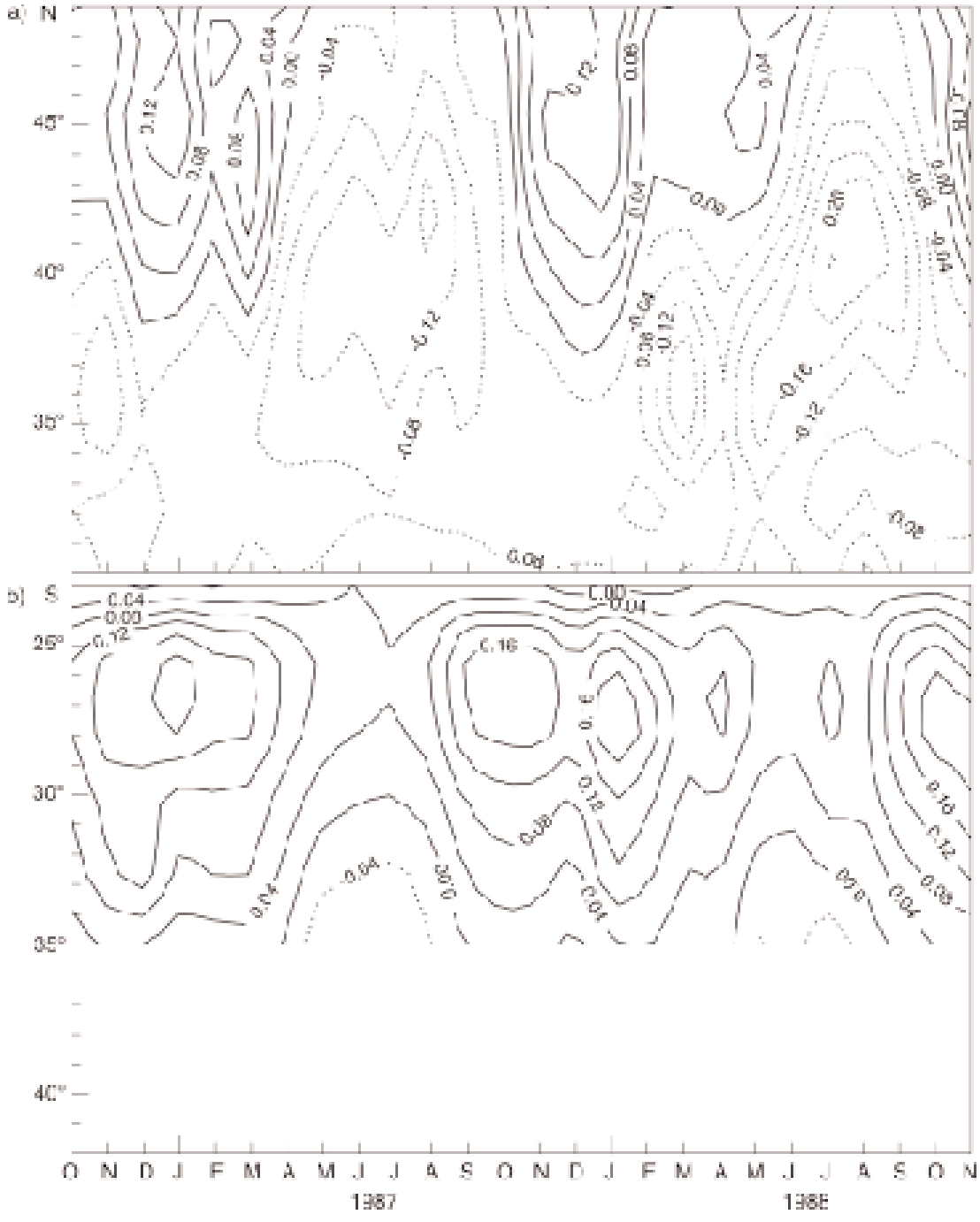

Fig 2: Monthly longshore wind stress during October 1986 through November 1988, calculated from ECMWF surface wind fields, for (a) the California Current and (b) the Benguela system. Contour intervals are 0.04 $N \cdot m^{-2}$. Positive values are towards the north in both cases

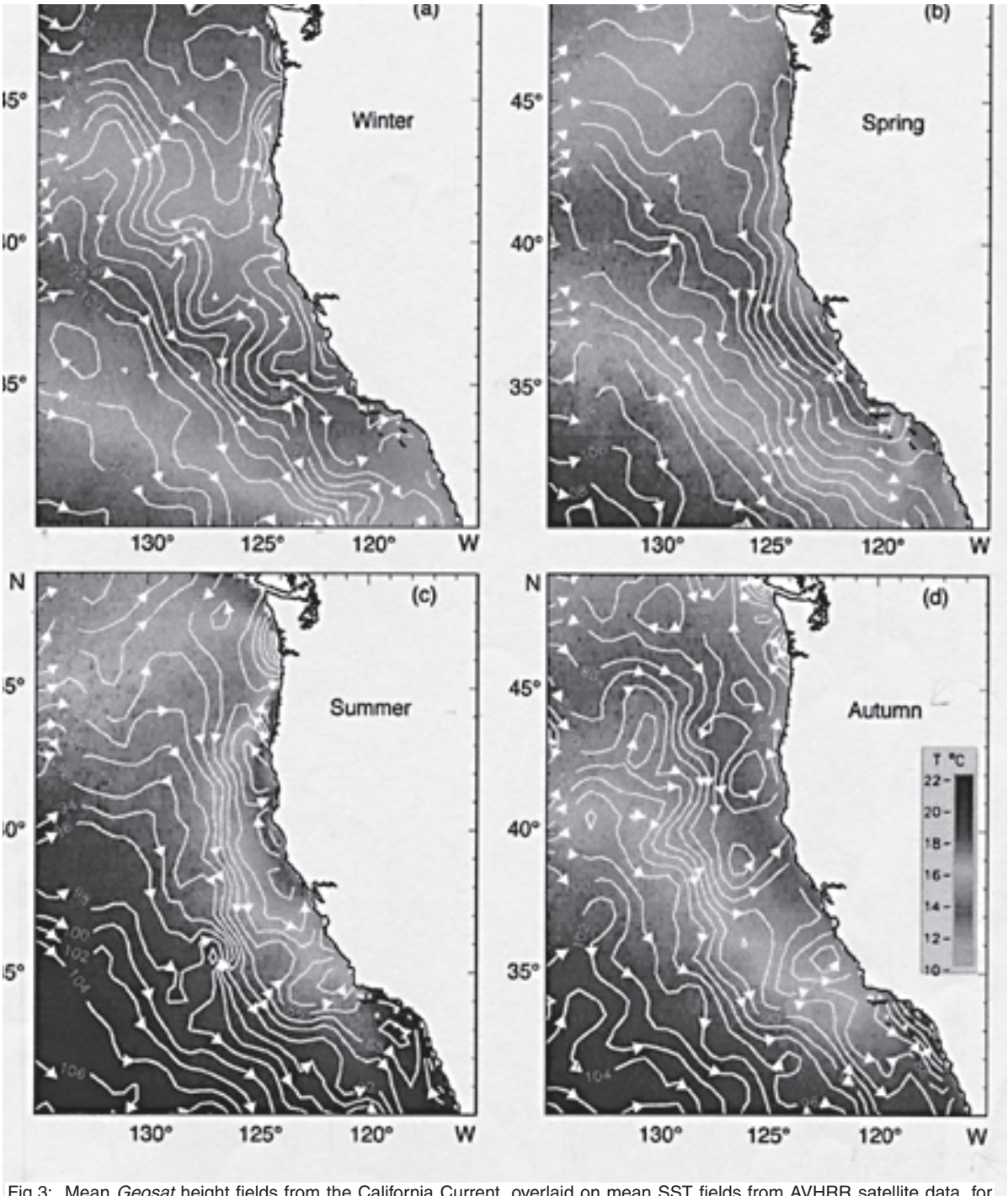

Fig 3: Mean *Geosat* height fields from the California Current, overlaid on mean SST fields from AVHRR satellite data, for (a) winter, (b) spring, (c) summer and (d) autumn. The long-term average dynamic height from Figure 1 is added to the altimeter data to replace the two-year mean altimeter height field that has been removed to eliminate the marine geoid. Contour intervals are 2 cm. Winter is defined as January–March, spring as April–June, summer as July–September and autumn as October–December

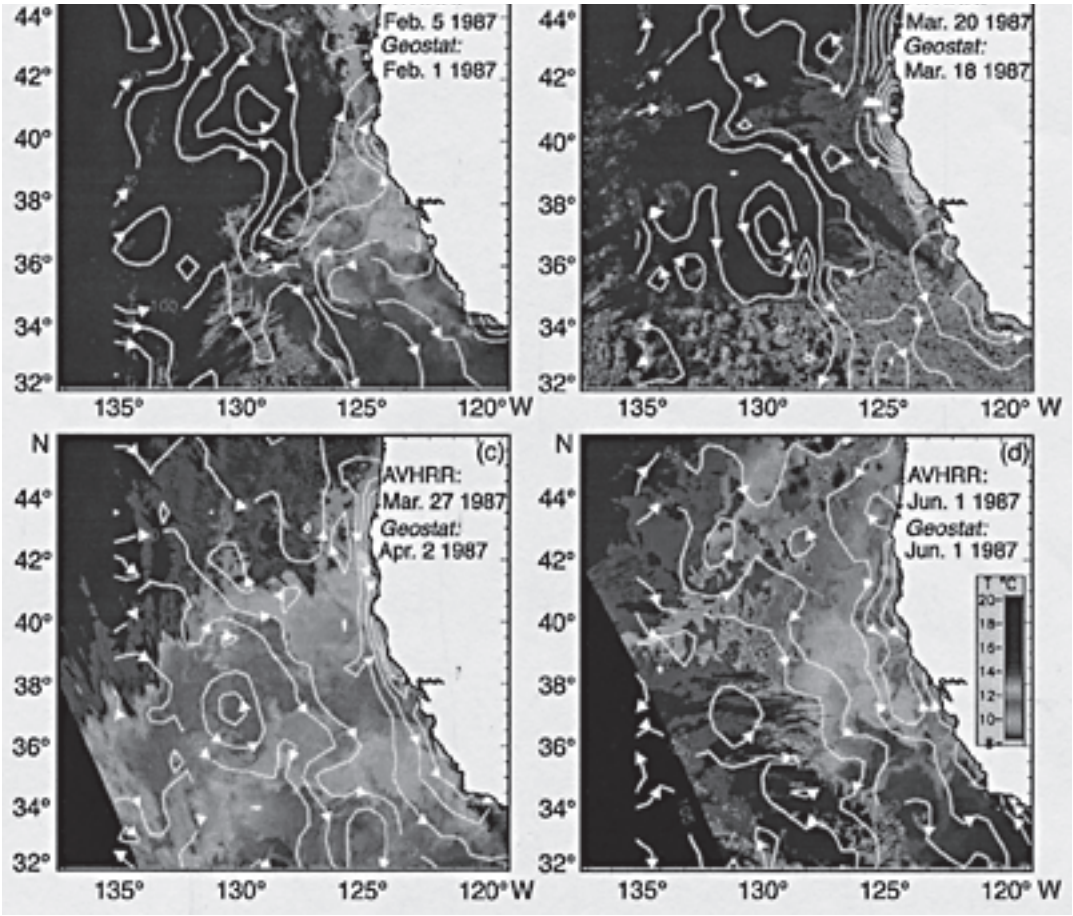

Fig 4: Altimeter height fields from individual *Geosat* 17-day cycles, overlaid on individual AVHRR SST fields over the California Current during 1987. Contour intervals are 5 cm

each spring or summer, flow along the entire West Coast is characterized by an equatorward current, concentrated in a relatively narrow jet. The equatorward flow is seen in Figure 3b, but the concentration into the jet is not evident in the mean spring altimeter height field. This may be the result of the variability between the two springs represented by this field (1987 and 1988).

The summer sea surface height field in Figure 3c consists of a concentrated equatorward jet that extends, at a distance of 100–500 km from the coast, from Oregon to southern California, where it enters the southern end of a cyclonic gyre that fills the Southern California Bight. Field data suggest that this jet develops near the coast in spring and moves offshore in summer. The jet remains closer to the coast off Oregon and Washington, but meanders far offshore of the California coast (Brink and Cowles 1991, Strub and James 1995). The altimeter data capture the offshore equatorward jet south of 43°N, but produce an unrealistic pattern next to the coast north of that; a northward cell off Oregon and a southward cell off Washington. This pattern is believed to be an artifact of the *Geosat* sampling, which consists of lines that cross the coast in the centre of those two cells (at approximately 44.5 and 46.2°N). In late summer, poleward flow appears next to the coast, as documented in a number of studies (Strub *et al*. 1987, Chelton *et al*. 1988, Largier *et al*. 1993). This poleward flow is suggested in the summer and autumn patterns shown

in Figures 3c and 3d, as the Davidson Current re-establishes itself.

The SST fields in winter and spring generally consist of zonal bands in Figure 3, resulting from the north-south gradient of seasonal heating. As water is warmed in the north in spring and summer, upwelling keeps the water colder in the region next to the coast. The equatorward jet occurs along the density front that coincides with the edge of this colder water. Both the front and the jet continue to move offshore in autumn. The jet remains evident in the height field in winter (Fig. 3a), although the SST front disappears presumably as a result of continued surface cooling.

The development from winter downwelling to summer upwelling conditions in 1987 is shown by individual altimeter and SST fields in Figure 4. At the beginning of February 1987, the poleward Davidson Current carries warm water north of 38°N (Fig. 4a). After a period of strong poleward winds in March (Fig. 2), sea levels next to the coast are high and currents are strongly polewards (Fig. 4b). This is followed by a large-scale change to equatorward winds (Fig. 2), low sea levels near the coast and a nearshore equatorward jet (Fig. 4c), extending from 45°N to southern California. This jet moves offshore on the outer edge of colder water in early June (Fig. 4d). The SST and surface height fields from winter and spring of 1988 (not shown) differ from those in 1987 in that poleward currents persist north of 42°N until June, mirroring the distribution of longshore winds in Figure 2. However, by late June, winds, SST and height fields demonstrate that the upwelling system extends the length of the California Current system. Strub and James (1995) present the altimeter and SST fields from later in summer for both 1987 and 1988, showing that a large-scale jet extended from Oregon and Washington to southern California in each of the summers. The fields discussed here document the evolution of the circulation from winter to summer in each of these years and show that the timing of the appearance of the equatorward jet follows the beginning of equatorward winds in a regional sense. However, after winds become upwelling-favourable all along the coast, the large-scale jet and eddy system appears similar in both years, moving offshore and becoming more convoluted with time.

Figure 5 shows contours of cross-track geostrophic velocity variances for each season from three years of TOPEX altimeter data. These velocity anomaly variances are the mean square differences between the values of the cross-track velocities from each cycle and the two-year mean, averaged over each of the four seasons. The variances therefore represent an estimate of the seasonally varying kinetic energy (KE) fields. They would be identical to KE if the velocity fluctuations were isotropic. Similar fields from the *Geosat* altimeter data show the same development in spring and summer, but the noisier *Geosat* data produce higher levels of variance in the quiet offshore areas and in the quieter winter period. The TOPEX data clearly show a general pattern of low energy offshore, whereas higher energy begins to be evident near the coast in spring, as the equatorward jet develops. This energy is maximum in midsummer (values >600 $cm^2 \cdot s^{-2}$), when the energetic jet has moved offshore with velocities 0.5-1 $m \cdot s^{-1}$. The centre of the KE maximum remains at approximately 127°W in summer, autumn and winter, whereas the area of the maximum KE diffuses out and maximum values dissipate to <100 $cm^2 \cdot s^{-2}$ in the offshore region in spring. The seasonal development of high energy next to the coast, inshore of low energy offshore, will be seen to be a major difference in comparison to the Benguela. The California Current system exists within an "eddy desert" and contributes eddy energy to the deep ocean, whereas the Benguela exists near an "eddy floodplain", i.e. the source of strong deep-ocean eddies in the Agulhas Retroflection.

Circulation in the Benguela system

The mean seasonal *Geosat* (plus climatological) height fields off South Africa are overlaid on seasonal SST in Figure 6. The method of using EOFs to filter out incoherent variance and to produce smoother seasonal cycles cannot be used in the Benguela system, because the variance and EOFs in that domain are dominated by the energetic Agulhas Retroflection. Therefore, the seasonal fields constructed from the EOFs in the region north of 34°S are nearly identical to the climatological height field in all seasons, showing a lack of contribution from the altimeter data. The seasonal mean *Geosat* height fields shown in Figure 6 resolve more structure in the region of the Benguela Current, although the nearshore fields should be interpreted cautiously (based on experience in the California Current system). Nevertheless, these seasonal height and SST fields provide a synoptic view of the circulation unavailable from traditional methods, as long as the limitations of the *Geosat* data are kept in mind.

Considering first the region north of 33°S, the broad, climatological equatorward flow in Figure 1 is shown by the altimeter data to be more concentrated and convoluted at a distance of about 300–500 km from the coast in summer (north of 34°S) and autumn (north of 30°S). It should be noted that the contour intervals are larger (4 cm) in Figure 6 than in Figures 1 and 3. The colder band of upwelled water next to the

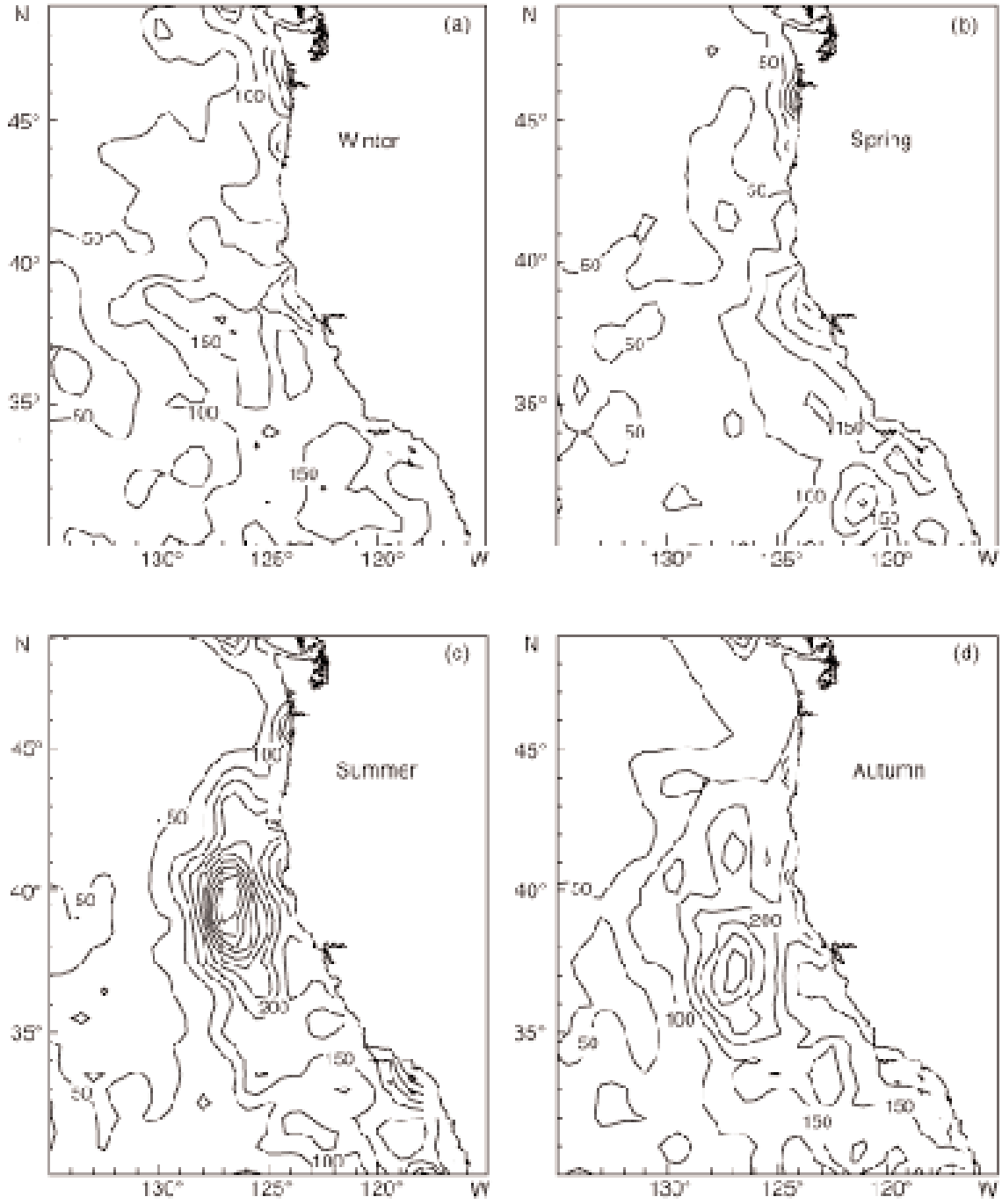

Fig 5: Seasonal cycle of cross-track geostrophic velocity variance from the California Current during the two-year *Geosat* period for (a) winter, (b) spring, (c) summer and (d) autumn. Contour intervals are 50 $cm^2 \cdot s^{-2}$

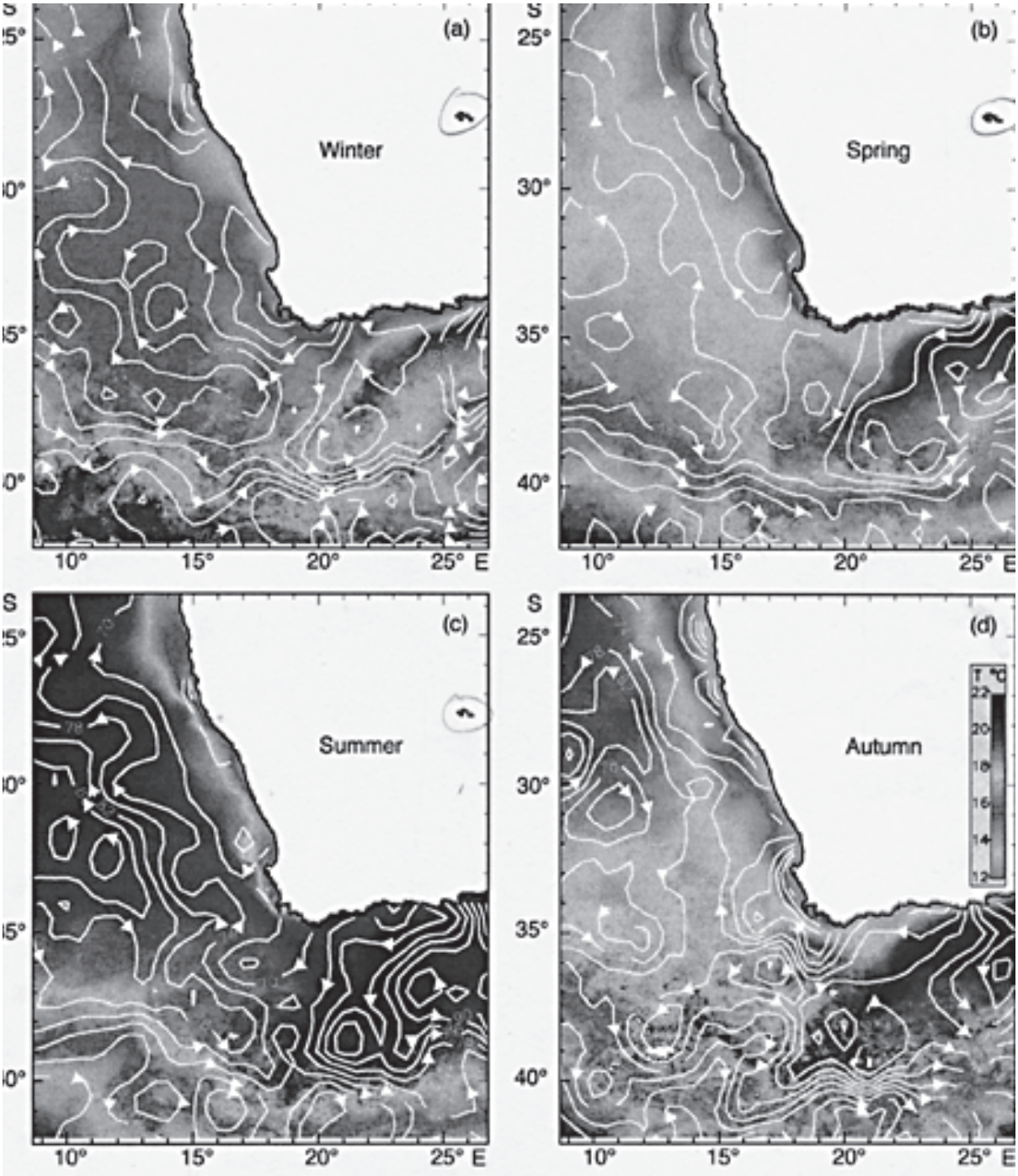

Fig 6: Mean *Geosat* height fields from the Benguela Current, overlaid on mean SST fields from AVHRR satellite data, for (a) winter, (b) spring, (c) summer and (d) autumn. Note that contour intervals are 4 cm (larger than in Figs 1 and 3). Winter is defined as July–September, spring as October–December, summer as January–March and autumn as April–June

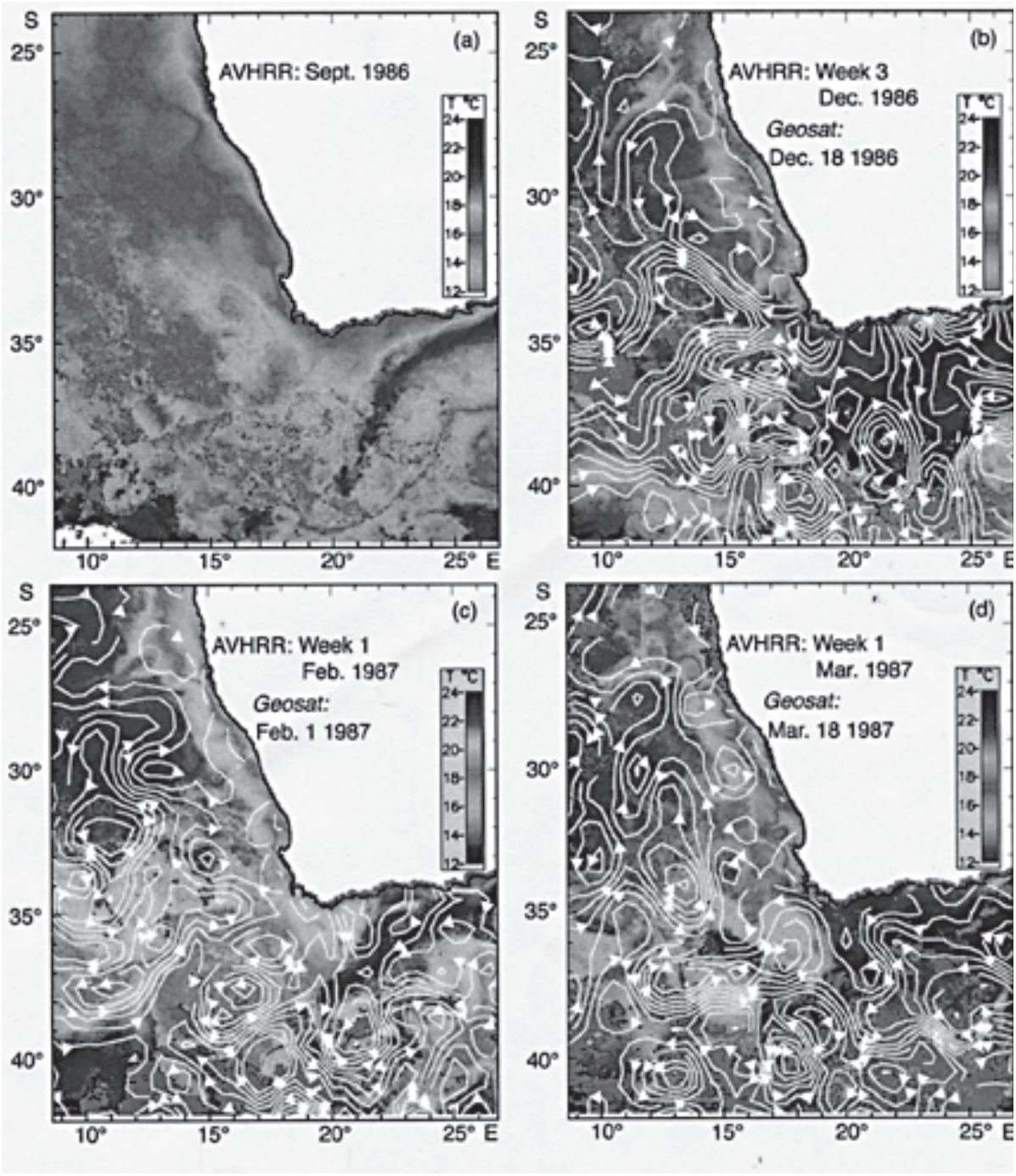

Fig 7: Altimeter height fields from individual cycles, overlaid on individual AVHRR SST fields over the Benguela Current during 1986–1987. Contour intervals are 5 cm and note changes in the colour bar

coast is narrower around 27–28°S, inshore of an anticyclonic meander that appears in the summer flow. A cyclonic meander is found north of this. This pair of anticyclonic and cyclonic meanders appears to pull filaments offshore in the vicinity of Lüderitz and moves south by about two degrees in winter. EOF analysis of 10 years of satellite SST data by Weeks and Shillington (1996) is consistent with this pattern, showing a warm anomaly near the coast between 27–28°S in summer and a cold anomaly in the same location in winter, which would be explained by a seasonal north-south movement of the anticyclonic-cyclonic meander pair. The tendency for anticyclonic flow during summer in that region may be influenced by the topography, because the shelf narrows between 27–28°S, compared to its width farther north and south, producing an anticyclonic tendency for any flow that follows the topography on its northward path.

North of 30°S, winds are upwelling-favourable and sea surface heights remain low in a region next to the coast all year. The equatorward winds (Fig. 2) and lower sea surface heights expand to the south in spring and summer. In the region within 200 km of the coast, the SST gradient is strongest and closest to the coast in summer, expanding offshore in autumn and winter and contracting in spring. *In situ* observations show a strong northward jet along this temperature front, similar to the equatorward jet found along the temperature front in the California Current. Although the contours of altimeter heights do not resolve a continuous jet along the temperature front, they place height contours along the front at scattered locations (i.e. off the Western Cape between 33 and 34°S in summer, between 32 and 34°S in autumn, and at various locations between 25–30°S in most seasons). Off the Cape Region (south of 32°S), the altimeter data show stronger equatorward flow (height gradients) in autumn and winter. Experience in the interpretation of *Geosat* altimeter data in other eastern boundary currents suggests that the altimeter fails to resolve stronger flow along the temperature front when it is closer to the coast in summer south of 32°S and picks up the current when it moves farther offshore in autumn and winter. The flow off the Cape Region is further complicated by the passage of strong eddies that are not averaged out in the short, two-year altimeter record, creating features that would not occur in the seasonal cycle formed from a longer record.

During the period of the best *Geosat* coverage (1987–1988), a strong spring transition is not found in the satellite altimeter data north of 30°S, where winds are upwelling-favourable all year. The seasonal transition south of 30°S is as described above: the development of the strong thermal front closest to the coast in summer, with implied equatorward flow that the altimeter does not sample well, followed by the offshore movement of the SST front and altimeter height gradient in autumn along the Cape Region (perhaps analogous to the much larger seasonal jet in the California Current). The strengthening of the meandering equatorward flow 300–500 km offshore north of 34°S in summer appears to be attributable to two types of process: cyclonic features develop in the upwelling region next to the coast and move offshore, lowering dynamic heights inshore of the jet; whereas anticyclonic features with high steric heights originate as cut-off rings and eddies in the Agulhas Retroflection area and move north, raising the dynamic heights on the offshore side of the jet.

These two processes are illustrated by a sequence of individual weekly SST fields and altimeter height fields centred on periods from September 1986 to March 1987. Figure 7a presents the SST field from the fourth week in September. No altimeter fields are available at that time. A large body of warm water is found west of the Cape Region, which is interpreted as water from the Agulhas Retroflection. Other features in the SST field include a warm tongue of water in the Agulhas Retroflection, a strong subtropical temperature front east of 19°E, and a complex SST pattern south of the Cape Region.

Altimeter heights centred on 18 December 1986 and the SST field from the third week in December 1986 are combined in Figure 7b. Considering the simpler region north of 32°S, a cold SST filament stretches south-west from 26 to 28°S, where the altimeter data indicate a meandering (cyclonic) equatorward flow around the filament. This meander is strengthened by the anticyclonic patterns to the south and west of the filament. Two other cyclonic features are shown at 200 km next to the coast in Figure 7b, and near 32–33°S, 16°E and 30°S, 14°E. These combine with strong anticyclonic flow around an elongated high near 33–34°S, 12–14°E to produce an intensive flow to the north-west, away from the Cape Region. This warm, anticyclonic high appears to be the warm feature identified in Figure 7a as a cut-off high from the Retroflection Region. On the southern flank of this high, flow is to the north-east, providing a path for colder water to move from 38–40°S, 8–10°E to just west of the Cape Region (34°S, 15–16°E). In this manner, the cut-off Agulhas eddy provides an anticyclonic transport path that carries water far offshore from the Cape Region and replaces it with water from much farther south, processes discussed by Lutjeharms and Valentine (1988), Lutjeharms and Van Ballegooyen (1988), Shannon *et al.* (1990), Lutje-

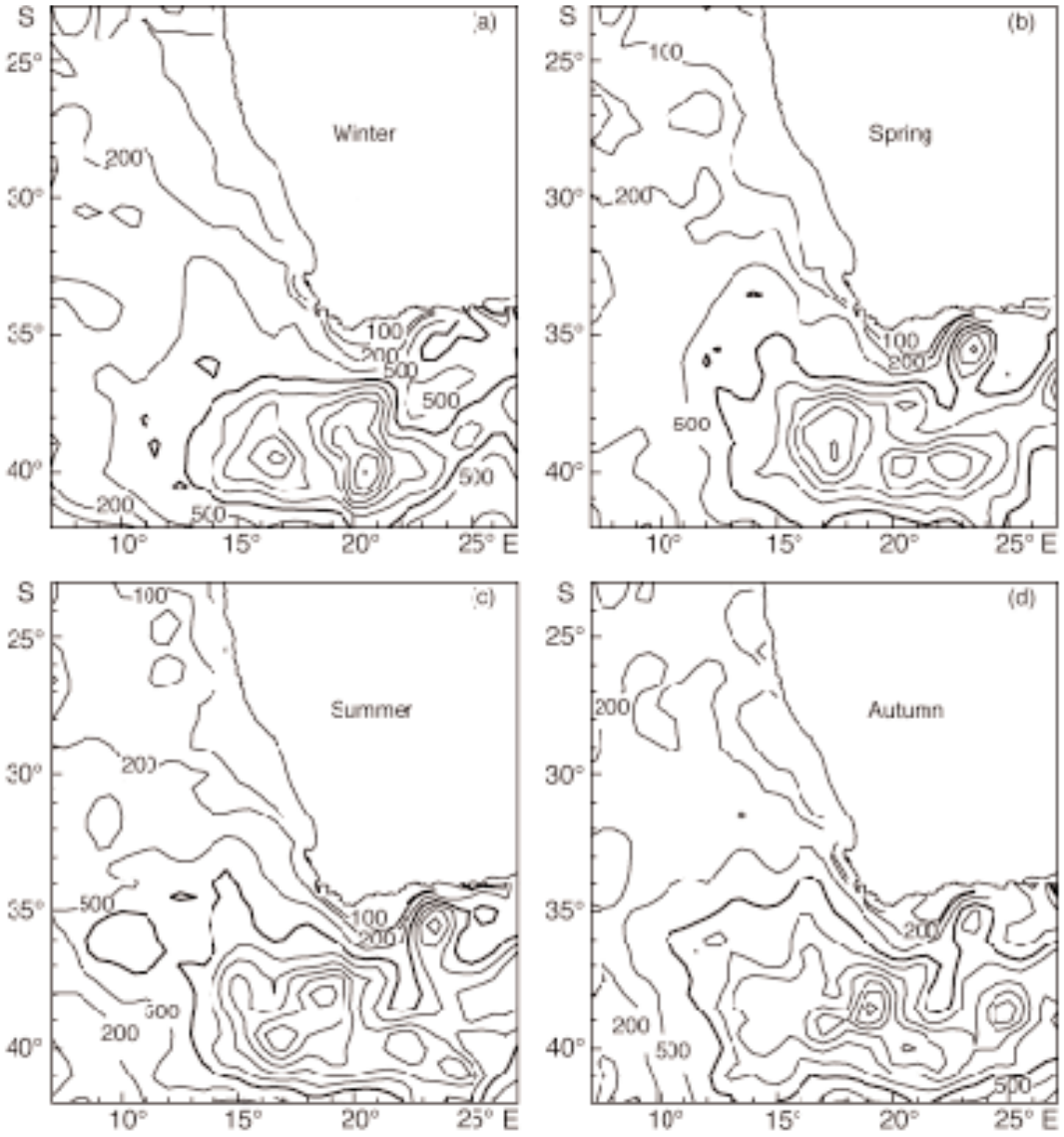

Fig 8: Seasonal cycle of cross-track geostrophic velocity variance from the Benguela Current during the two-year *Geosat* period for (a) winter, (b) spring, (c) summer and (d) autumn. Contour intervals are 500 $cm^2 \cdot s^{-2}$, except for initial intervals of 50, 100 and 200 $cm^2 \cdot s^{-2}$

harms *et al*. (1991), Duncombe Rae *et al.* (1992), Gründlingh (1995), and others.

Figures 7c and 7d present altimeter and SST fields for periods in January/February and March 1987. Part of the elongated anticyclonic high evident in Figure 7b moves to the north-west in Figure 7c (centred at 32°S, 11°E) and Figure 7d (29–30°S, 8–9°E), whereas other parts of the high remain off the Cape Region. During the same period, the two cyclonic features that were 200 km from the coast at 30°S and 32–33°S (Fig. 7b) strengthen to become closed cyclonic eddies. The combination of raised heights offshore and lowered heights inshore in the cyclonic eddies results in an intensified meandering current,

leading north-west from the Cape Region in February (Fig. 7c). This current links the Cape Region to the Lüderitz filament. Transports toward and away from the Cape Region are affected by these large and persistent offshore mesoscale features. In March (Fig. 7d), the flow away from the Cape Region is to the south-west, then west to 37°S, 12°E, around a large anti-cyclonic feature. The pair of cyclonic (36°S, 16–17°E) and anticyclonic (38°S, 15–16°E) eddies south-west of the Cape persists from December to February.

The eddy at 33°S, 15°E in Figure 7c demonstrates how a cyclonic eddy can appear to have a warm core. Cold water has a direct path from around 38°S, 12°E to the Cape Region (34°S, 17°E), where it merges with warm water brought from the east. It can then flow to the north-west in the meandering path between the cyclonic lows (inshore) and anti-cyclonic highs (offshore). Although the cyclonic eddy at 33°S, 15°E in Figure 7c began in the cooler upwelling region next to the coast in December, by February it is farther offshore in warmer water. Field surveys reported by Lutjeharms and Van Ballegooyen (1988) have shown that tongues of warm water off South-West Africa are caused by intrusions from the Agulhas Retroflection that are generally only 50–100 m deep. This thin upper layer of warm water may hide deeper features of the circulation from satellite IR images, without drastically changing the surface dynamic height. As it sits in the warmer surface water, the cyclonic eddy can draw cooler water from the south around itself in a clockwise direction, creating the appearance of a warm core cyclonic eddy, as shown in Figures 7c and 7d. This eddy persists through May and continues to move offshore. Combining the altimeter and SST data helps to avoid misinterpretations of the SST data, which might have resulted in a conclusion that all warm features are anticyclonic. The altimeter data also make it clear that cyclonic eddies (in addition to the anticyclonic eddies) are important features in the circulation around the Agulhas Retroflection, the Subtropical Front and the Benguela system.

Contours of seasonal geostrophic velocity variance for the Benguela and Agulhas regions are presented in Figure 8, similar to those in Figure 5. It should be noted, however, that the contour interval is 50 $cm^2 \cdot s^{-2}$ in Figure 5, with maximum values of about 600 $cm^2 \cdot s^{-2}$ offshore of the California Current system in summer. Contour intervals vary in Figure 8 to allow depiction of maximum values in the Agulhas of 3 500 $cm^2 \cdot s^{-2}$. Concentrating on the Benguela Current north of 32°S, maximum velocity variance values of only 200 $cm^2 \cdot s^{-2}$ are found about 300 km from the coast in spring and summer, with no indication of a seasonal offshore movement. This region of high variability is assosiated with the changing position of the meandering flow around the Lüderitz upwelling centre and filament. Off the Cape Region, the 500 $cm^2 \cdot s^{-2}$ contour moves closer to the coast between winter and spring and the 1 000 $cm^2 \cdot s^{-2}$ contour moves closer to the coast in summer and autumn, indicating an increase in variance that may be associated with offshore movement of the front and jet picked up by the TOPEX altimeter in summer and autumn. However, as noted before, this region is complicated by the passage of eddies from the Agulhas Retroflection.

Looking farther south at the Agulhas Retroflection in Figure 8, the areas of high variability (values >1 000 $cm^2 \cdot s^{-2}$, shown as the dark contour) are most contracted in winter, expanding to the north-west in summer and autumn. The seasonal variation in the surface height field in Figure 6 shows steeper gradients along the Subtropical Front west of 20°E in summer and autumn, than in winter, with greater convolutions in autumn. A longer time-series of high-resolution altimeter data is needed to determine if this pattern represents a normal seasonal development.

CONCLUSIONS

- Although wind-driven coastal upwelling processes are believed to be similar in the Benguela and California Current systems, altimeter and SST data reveal differences in the manner the large-scale circulation of the two systems interacts with the surrounding basin.
- In the California Current, a seasonal, offshore migrating jet develops each spring and summer, which delivers eddy kinetic energy to the deep ocean.
- In spring and summer, the jet forms a continuous path from north to south in the California Current system.
- The timing of the formation of the jet in each region of the California Current system depends on the winds, with interannual variability.
- In the Benguela Current north of the Cape Region, a convoluted jet is found several hundred kilometres offshore and is stronger in the summer.
- Upwelling occurs all year north of 32°S and the offshore jet does not appear to migrate offshore in a regular fashion.
- The strengthening of the jet in summer is caused by injection of water with high steric heights from the Agulhas Current on the offshore side of the jet and by upwelled water with low steric heights on the inshore side of the jet.

- Upwelling off the Cape Region (32–34°S) appears more seasonal in SST, but the Geosat data do not resolve the circulation in this region well. At times, it appears that cyclonic eddies originate at the coast and propagate offshore to the west.
- The Cape Region is forced by both cyclonic and anticyclonic eddies that are stronger than those found in the California Current. These create complex transport paths from the coast near the Cape Region to the deep ocean, with time-scales of several months.

ACKNOWLEDGEMENTS

The work of PTS and CJ was supported by Grant 958128 from the Jet Propulsion Laboratory, Grants NAGW–2475 and NAGW–4596 from NASA, and ONR Grant N00014–92–J–1631. The work of FAS and SJW was supported by the Benguela Ecology Programme and the University of Cape Town. Altimeter and AVHRR data over the California Current were obtained from the Jet Propulsion Laboratory, Pasadena, California, USA., and Ocean Imaging. AVHRR data over the Benguela Current were obtained from the Space Applications Institute at the Joint Research Centre, Ispra, Italy.

LITERATURE CITED

BAKUN, A. and C. S. NELSON 1991 — The seasonal cycle of wind-stress curl in subtropical eastern boundary current regions. *J. phys. Oceanogr*. **21**: 1815–1834.

BRATSETH, A. M. 1986 — Statistical interpolation by means of successive corrections. *Tellus* **38A**: 439–447.

BRINK, K. H. and T. J. COWLES 1991 — The Coastal Transition Zone program. *J. geophys. Res*. **96**(C8): 14637–14647.

CHELTON, D. B., BRATKOVICH, A. W. BERNSTEIN, R. L. and P. M. KOSRO 1988 — Poleward flow off central California during spring and summer of 1981 and 1984. *J. geophys. Res*. **93**(C9): 10604–10620.

DUNCOMBE RAE, C. M., SHILLINGTON, F. A., AGENBAG, J. J., TAUNTON-CLARK, J. and M. L. GRÜNDLINGH 1992 — An Agulhas ring in the South Atlantic Ocean and its interaction with the Benguela upwelling frontal system. *Deep-Sea Res*. **39**(11A/12A): 2009–2027.

GRÜNDLINGH, M. L. 1995 — Tracking eddies in the southeast Atlantic and southwest Indian Oceans with TOPEX/POSEIDON. *J. geophys. Res*. **100**(C12): 24977–24986.

HICKEY, B. M. 1998 — Coastal oceanography of Western North America from the tip of Baja California to Vancouver Island. *The Sea* **11**: 345–393.

HUTCHINGS, L. 1992 — Fish harvesting in a variable, productive environment – searching for rules or searching for exceptions? In *Benguela Trophic Functioning*. Payne, A. I. L., Brink, K. H., Mann, K. H. and R. Hilborn (Eds). *S. Afr. J. mar. Sci*. **12**: 297–318.

LARGIER, J. L., MAGNELL, B. A. and C. D. WINANT 1993 — Subtidal circulation over the northern California shelf. *J. geophys. Res*. **98**(C10): 18147–18179.

LENTZ, S. J. 1992 — The surface boundary layer in coastal upwelling regions. *J. phys. Oceanogr*. **22**: 1517–1539.

LEVITUS, S. and R. GELFELD 1992 — *NODC Inventory of Physical Oceanographic Profiles*. Key to Oceanography Records Documentation, No. 18. Washington D.C., U.S. Government Printing Office: 242 pp.

LUTJEHARMS, J. R. E. and J. M. MEEUWIS 1987 — The extent and variability of South-East Atlantic upwelling. *In The Benguela and Comparable Ecosystems*. Payne, A. I. L., Gulland, J. A. and K. H. Brink (Eds). *S. Afr. J. mar. Sci*. **5**: 51–62.

LUTJEHARMS, J. R. E., SHILLINGTON, F. A. and C. M. DUNCOMBE RAE 1991 — Observations of extreme upwelling filaments in the Southeast Atlantic Ocean. *Science* **253**(5021): 774–776.

LUTJEHARMS, J. R. E. and H. R. VALENTINE 1988 — Evidence for persistent Agulhas rings south-west of Cape Town. *S. Afr. J. Sci*. **84**(9): 781–783.

LUTJEHARMS, J. R. E. and R. C. VAN BALLEGOOYEN 1988 — The retro-flection of the Agulhas Current. *J. phys. Oceanogr*. **18**(11): 1570–1583.

LYNN, R. J. and J. J. SIMPSON 1987 — The California Current system: the seasonal variability of its physical characteristics. *J. geophys. Res*. **92**(C12): 12947–12966.

PARRISH, R. H., BAKUN, A., HUSBY, D. M. and C. S. NELSON 1983 — Comparative climatology of selected environmental processes in relation to eastern boundary current pelagic fish reproduction. In *Proceedings of the Expert Consultation to Examine Changes in Abundance and Species Composition of Neritic Fish Resources, San José, Costa Rica, April 1983.* Sharp, G. D. and J. Csirke (Eds). *F.A.O. Fish. Rep*. **291**(3): 731–777.

SHANNON, L. V. 1985 — The Benguela ecosystem. 1. Evolution of the Benguela, physical features and processes. In *Oceanography and Marine Biology. An Annual Review* **23**. Barnes, M. (Ed.). Aberdeen; University Press: 105–182.

SHANNON, L. V., AGENBAG, J. J., WALKER, N. D. and J. R. E. LUTJEHARMS 1990 — A major perturbation in the Agulhas retroflection area in 1986. *Deep-Sea Res*. **37**(3): 493–512.

SHILLINGTON, F. A. 1998 — The Benguela upwelling system off southwestern Africa. *The Sea* **11**: 583–604.

SMITH, R. L. 1983 — Circulation patterns in upwelling regimes. In *Coastal Upwelling, its Sediment Record*. Suess, E. and J. Thiede (Eds). New York; Plenum: 13–35.

STRUB, P. T., ALLEN, J. S., HUYER, A., SMITH, R. L. and R. C. BEARDSLEY 1987 — Seasonal cycles of currents, temperatures, winds, and sea level over the northeast Pacific continental shelf: 35°N to 48°N. *J. geophys. Res*. **92**(C2): 1507–1526.

STRUB, P. T. and C. JAMES 1988 — Atmospheric conditions during the spring and fall transitions in the coastal ocean off western United States. *J. geophys. Res*. **93**(C12): 15561–15584.

STRUB, P. T. and C. JAMES 1995 — The large-scale summer circulation of the California current. *Geophys. Res. Letts* **22**: 207–210.

VAZQUEZ, J., ZLOTNICKI, V. and L-L. FU 1990 — Sea level variabilities in the Gulf Stream between Cape Hatteras and 50°W: a Geosat study. *J. geophys. Res*. **95**(C10): 17957–17964.

WEEKS, S. J. and F. A. SHILLINGTON 1996 — Temporal and spatial variability of the physical characteristics of the southern Benguela upwelling system. Programme and Abstracts of the Benguela Dynamics. Impacts of Variability on Shelf-Sea Environments and their Living Resources Symposium, November 1996, Cape Town: p. 76.

ZLOTNICKI, V., HAYASHI, A. and L-L. FU 1990 — *The JPL-Oceans 8902 Version of Geosat Altimetry Data*. Internal Document, Jet Propulsion Laboratory, California Institute of Technology, Pasadena, California **D-6939**: 46 pp.